

Sintering of the mechanically activated MgO-TiO₂ system

S. Filipovic^a, N. Obradovic^{a,*}, D. Kosanovic^a, V. Pavlovic^a, A. Djordjevic^b

^aInstitute of technical sciences SASA, Knez Mihailova 35/IV 11000 Belgrade, Serbia

^bSchool of Electrical Engineering, University of Belgrade, Bulevar kralja Aleksandra 73, 11000 Belgrade, Serbia

Mixtures of MgO-TiO₂ powders were mechanically activated in a planetary ball mill for a time interval from 0 to 120 minutes. The influence of the mechanical activation on the phase composition and crystal structure have been analyzed by X-ray diffraction (XRD), while the effect of the activation and sintering process on the microstructure was investigated by scanning electron microscopy (SEM). Using the data obtained from XRD microstructural parameters, the volume averaged crystallite size (D), the density of dislocations (ρ_D) and the lattice strain (ϵ_{hkl}) values were calculated. Dielectric measurements were performed in order to show the variations in the dielectric constant as a function of the time of mechanical activation.

Key words: Magnesium-titanate, Mechanical activation, XRD, Electrical properties.

Introduction

Much research in the last decade has studied dielectric materials, mainly because of the rapid progress in communication systems, such as cellular phones, satellites and global positioning systems. Usage of materials for these purposes requires ceramics with a dielectric constant of 10-20, an extremely low dielectric loss, and a low-cost [1, 2]. Materials that meet appropriate properties for these applications are certainly the binary magnesium titanates, MgTiO₃ and Mg₂TiO₄ [3, 4]. These compounds have dielectric constants of 16 and 14, respectively. Moreover, the molar ratio of these phases has an influence on dielectric constant [5]. The conditions and synthesis method greatly affects the dielectric properties [6]. Extensive research revealed that mechanical activation could simplify or accelerate the solid-state reaction, which normally occurs at high temperature and/or high pressure. High-energy ball milling has many advantages, such as simplicity, a relatively inexpensive production of nano-sized powders, applicability to any class of materials, etc. During mechanical activation, powder particles are subjected to severe plastic deformation that results in the formation of a high concentration of defects. This induces enhanced atomic mobility; promotes different phenomena depending on the materials being milled [7].

In this study, the effects of mechanical activation on the phase composition, microstructure and dielectric constant of a sintered MgO-TiO₂ system were investigated.

Experimental

Mixtures of MgO (99% Sigma-Aldrich) and TiO₂ powders (99.8% Sigma-Aldrich) at a molar ratio MgO:TiO₂ = 2:1 were mechanically activated by grinding in a high energy planetary ball mill (Retsch type PH 100). The milling process was performed in air for 5, 10, 20, 40, 80 and 120 minutes at a basic disc rotation speed of 400 rpm. The ball-to-powder mixture mass ratio was 20:1. Samples were denoted as MT0 to MT120 according to the milling time. The binder-free powders were compacted using a uniaxial double action pressing process in an 8 mm diameter tool (hydraulic press RING, P-14, VEB THURINGER). Compacts were placed in an alumina boat and heated in a tube furnace (Lenton Thermal Design Typ 1600). Compacts were sintered isothermally at 1300 °C in an air atmosphere for 2 hours and a heating rate of 10 Kminute⁻¹.

X-ray powder diffraction patterns after milling and the thermal treatment were obtained using a Philips PW-1050 diffractometer with λ Cu-K α radiation and a step/time scan mode of 0.05 ° s⁻¹.

The morphology of the powders obtained after heating was characterized by scanning electron microscopy (JEOL JSM-6390 LV). The pellets were cracked and covered with gold in order to perform these measurements.

Measurement of the dielectric properties was performed on a network analyzer Agilent E5062A in the range 50-500 MHz, on sintered specimens coated with silver electrodes.

Results and Discussion

It is well known that a mechanical treatment leads to a decrease in crystal size, introduction of structural defects, amorphisation, chemical reactions, etc [8]. X-

*Corresponding author:
Tel : +381-11-2027203
Fax: +381-11-2185263
E-mail: nina.obradovic@itn.sanu.ac.rs

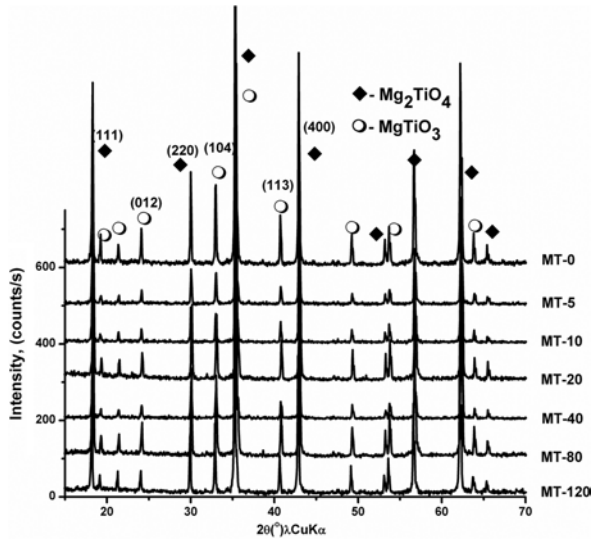


Fig. 1. XRD patterns of mixtures sintered at 1300 °C for 2 h.

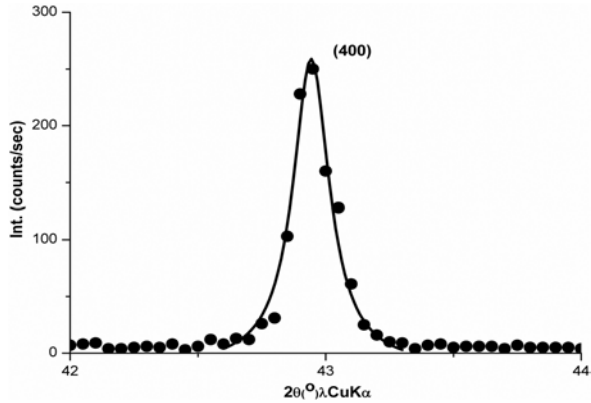


Fig. 2. XRD peak (●) for the (400) reflection of Mg_2TiO_4 fitting to a Lorentz function (line).

ray analysis of all the samples indicates the presence of two phases, $MgTiO_3$ and Mg_2TiO_4 , that were confirmed by JCPDS cards (79-0831 for $MgTiO_3$ and 79-0829 for Mg_2TiO_4), Fig. 1. Diffraction patterns showed very sharp and intensive reflections. This suggests that the processes of recrystallization and annihilation of structural defects during the sintering process were taking place.

Analysis of the broadening of Bragg reflections is a very convenient way to determine the size of crystalline domains from powder diffraction data [9]. The size of crystallites has been determined by application of Scherrer's equation:

$$D_{hkl} = k\lambda/\beta \cos \theta \quad (1)$$

where: D- crystallite size, k- Scherrer constant, λ - wavelength, β - integral breadth, and θ - angular peak position. Usually, a full width at half maximum (FWHM) instead of integral breadth is used, which brings mistakes in determining the size of crystalline domains. Taking all of this into consideration, we used the integral breadth in our calculation of microstructural parameters. First, peaks were fitted to a Lorentz function and the FWHMs obtained were used for the determination of a true value of β , as shown in Fig. 2 [9].

In Table 1 are given values of crystalline domain sizes calculated in two different ways, using the full width at half maximum (FWHM) and using the integral breadth (β). It can be noticed that values are significantly lower when using integral breadth.

Microstructural parameters obtained from Scherrer's method [10]: crystallite size (D), density of dislocations (ρ_D) and lattice strain (ϵ_{hkl}) are given in Table 2.

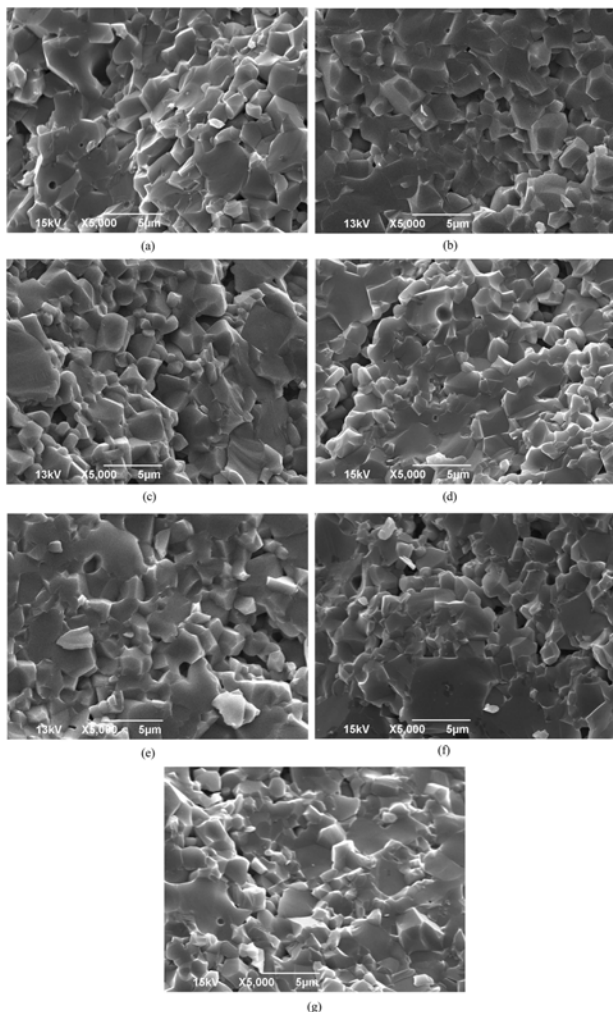
These calculations have been conducted for the most

Table 1. Comparison of D_{hkl} values calculated in different ways.

Sample	Phase	D_{hkl} (nm), using β						D_{hkl} (nm), using FWHM					
		104	113	012	111	220	400	104	113	012	111	220	400
MT0	$MgTiO_3$	62	49	71				97	77	111			
	Mg_2TiO_4				70	69	61				110	108	95
MT5	$MgTiO_3$	61	48	66				95	76	104			
	Mg_2TiO_4				50	53	49				78	83	77
MT10	$MgTiO_3$	55	60	70				86	93	111			
	Mg_2TiO_4				55	60	56				87	94	88
MT20	$MgTiO_3$	50	49	56				79	77	87			
	Mg_2TiO_4				55	58	54				86	91	86
MT40	$MgTiO_3$	52	35	48				82	54	76			
	Mg_2TiO_4				60	53	53				94	87	83
MT80	$MgTiO_3$	56	43	56				87	68	87			
	Mg_2TiO_4				53	64	55				84	101	86
MT120	$MgTiO_3$	65	57	57				103	89	90			
	Mg_2TiO_4				61	56	52				96	88	82

Table 2. Microstructural parameters obtained from Scherrer's method [10]:

Sample	Phase	D _{hkl} (nm)						ρ _D (10 ¹⁰ cm ⁻²)						ε _{hkl}						
		104	113	012	111	220	400	104	113	012	111	220	400	104	113	012	111	220	400	
MT0	MgTiO ₃	62	49	71				8	12	6				0.2	0.2	0.2				
	Mg ₂ TiO ₄				70	69	61				6	6	8				0.3	0.2	0.1	
MT5	MgTiO ₃	61	48	66				8	13	7				0.2	0.2	0.2				
	Mg ₂ TiO ₄				50	53	49				12	11	12				0.4	0.2	0.2	
MT10	MgTiO ₃	55	60	70				10	8	6				0.2	0.2	0.2				
	Mg ₂ TiO ₄				55	60	56				10	8	9				0.4	0.2	0.2	
MT20	MgTiO ₃	50	49	56				12	12	10				0.2	0.2	0.3				
	Mg ₂ TiO ₄				55	58	54				10	9	10				0.4	0.2	0.2	
MT40	MgTiO ₃	52	35	48				11	20	13				0.2	0.3	0.3				
	Mg ₂ TiO ₄				60	53	53				8	11	11				0.4	0.2	0.2	
MT80	MgTiO ₃	56	43	56				10	16	10				0.2	0.2	0.3				
	Mg ₂ TiO ₄				53	64	55				10	7	10				0.4	0.2	0.2	
MT120	MgTiO ₃	65	57	57				7	10	10				0.2	0.2	0.3				
	Mg ₂ TiO ₄				61	56	52				8	10	11				0.4	0.2	0.2	

**Fig. 3.** SEM micrographs of samples MT-0 (a), MT-5 (b), MT-10 (c), MT-20 (d), MT-40 (e), MT-80 (f), MT-120 (g)

intensive reflection, and a reflection with no overlapping. As can be noticed, the crystallite size decreases until an activation time of 40 minutes, after that an increase is observed. At the beginning of the milling process the dominant effect is grain fragmentation, which leads to a decrease in crystallite size even after sintering. Samples activated for a longer time, start to form agglomerates, as a tendency to reduce the surface free energy, and an amorphous phase during the mechanical treatment. This system has a greater amount of mechanical energy, inducing a greater system activity, increased mass transport and a larger crystal size after the thermal treatment. Beside this effect, greater changes in the microstructural parameters for MgTiO₃ phase can be observed.

Fig. 3. presents micrographs of samples sintered at 1300°C for 2 h. All the micrographs shown indicate a medium sintering stage along with enclosed but not spherical pores. There is a noticeable presence of two different phases in all samples, one with smaller polygonal shape grains (MgTiO₃), and more compact areas of Mg₂TiO₄. With a longer activation time, an increase in the amount of the spinel phase (Mg₂TiO₄), along with more compact samples can be seen. The presence of fractures between grains, which is probably due to the presence of agglomerates in the starting powders, was observed. At Fig. 3 (d), for sample MT-20, we can observe the presence of large crack between areas, which cause lower values of the electrical characteristic, as seen in Table 3.

Table 3. shows values of the dielectric constant, calculated from capacitance measurements. The evaluation of ε_r was performed in two ways: the first was using the classical equation that relates the geometrical dimensions

Table 3. Dielectric constant of sintered samples.

Sample	ϵ_r (classical)	ϵ_r (numerical)
MT-0	14.6	12.5
MT-5	17.1	15.5
MT-10	17.2	15.5
MT-20	17.0	15.3
MT-40	17.6	15.9
MT-80	18.6	16.9
MT-120	18.4	16.6

of a sample and its capacitance; the second one was numerical, using a program that simulates electrostatic systems [11]. The program takes into account the edge effects and stray capacitance. Hence, it yields lower values for ϵ_r .

The electrical measurements showed that the dielectric permittivity of these specimens increase with the activation time, reaching a maximum value for the sample activated for 80 minutes. As can be seen, there is no significant difference between samples MT-80 and MT-120, which confirms that we reached the optimal time of mechanical activation for this system. It is known that a greater density results in a higher dielectric permittivity owing to a lower porosity. Results presented in Table 3. are in accordance with the evaluated densities [7]. Also it is known from the literature data [5] that different ratio between the phases has an influence on ϵ_r values. Since our samples consist of two different phases and there is a difference in densities, changes in dielectric constant must be contributed to both factors.

Conclusions

In this paper, we investigated changes in the microstructural, phase composition and dielectric properties of MgO-TiO₂ system sintered at 1300 °C for 2 hours. XRD analyses confirmed the presence of two phases, a dominant spinel Mg₂TiO₄ and ilmenite MgTiO₃, also used for the calculation of the microstructural parameters. These data show greater changes for the MgTiO₃ phase.

Comparing results for D_{hkl} calculated using full width at half maximum (FWHM) instead of integral breadth, we noticed differences in values of about 35%. It was shown that the dielectric permittivity of this material increases with activation time in accordance with changes in the densities and phase compositions of sintered samples. Maximum values of both the density (about 94% ρ_i) and the dielectric constant were reached for the MT-80 sample. SEM analyses confirmed the presence of two phases, along with more compact samples for longer activation times.

Acknowledgement

This research was performed within project 172057 OI funded by the Ministry for Education and Science of the Republic of Serbia.

References

1. A. Belous, O. Ovchar, D. Durylin, M. Valant, M. Macek-Krzmanac, and D. Suvorov, *J. Eur. Ceram. Soc.* 27 (2007) 2963-2966.
2. E.A.V. Ferri, J.C. Sczancoski, L.S. Cavalcante, E.C. Paris, J.W.M. Espinosa, A.T. de Figueiredo, P.S. Pizani, V.R. Mastelaro, J.A. Varela, and E. Longo, *Mat. Chem. and Phys.* 117 (2009) 192-198.
3. Z. Li, S. Chun-Ying, and Q. Tai, *J. Inorg. Mater.* 26 (2011) 219-224.
4. A. Belous, O. Ovchar, D. Durilin, M. Macek-Krzmanac, M. Valant, and D. Suvorov, *J. Am. Ceram. Soc.* 89 (2006) 3441-3445.
5. E.S. Kim, and S.N. Seo, *J. Kor. Ceram. Soc.* 47 (2010) 163-168.
6. A.S. Khim, J. Wang, and X. Junmin, *J. of Alloys and Comp.* 311 (2000) 181-187.
7. S. Filipovic, N. Obradovic, V.B. Pavlovic, S. Markovic, M. Mitric, and M.M. Ristic, *Sci. Sint.* 42 (2010) 143-151.
8. V.P. Pavlovic, J. Krstic, M.J. Scepanovic, J. Dojcilovic, D. M. Minic, J. Blanusa, S. Stevanovic, V. Mitic, and V.B. Pavlovic, *Cer. Inter.* 37 (2011) 2513-2518.
9. C. Weidenthaler, *Nanoscale* 3 (2011) 792-810.
10. Lj. Karanovic, *Applied Crystallography*, Belgrade University, Belgrade, in Serbian (1996) 91.
11. M.M. Nikolic, A.R. Djordjevic, M.M. Nikolic, *ES3D: Electrostatic Field Solver for Multilayer Circuits*, Artech House, Boston (2007).